

X-RAY CHARACTERIZATION OF BONDING INTERFACES

F. Rieutord^{1,*}, H. Moriceau², B. Bataillon^{1,2}, C. Morales², J. Eymery¹

1- CEA-DRFMC, CEA Grenoble, 17 Rue des Martyrs, 38054 Grenoble Cedex 9 - France

2- CEA-DRT / LETI-DIHS, CEA Grenoble,

17 Rue des Martyrs, F38054 Grenoble Cedex 9 - France

*e-mail:rieutord@cea.fr

ABSTRACT

Interfacial X-ray reflection is used to study the evolution of bonding interfaces as a function of annealing. The sensitivity of the method allows the observation of very fine density or thickness changes in the different components of the interfacial profile. The example of Si/Si hydrophilic bonding is described in some details. Finally a direct method applicable to symmetric bonding (Si/Si or SiO₂/SiO₂) is used to obtain the electron density profile, removing possible uncertainties associated to the phase loss problem of X-ray scattering.

INTRODUCTION

Wafer bonding has been established as a technique suitable to produce sharp interfaces between different materials. However the exact structure of the interface at the different steps of the bonding process is poorly known, due to the difficulty of investigating such a narrow interface buried under macroscopic thickness of material. Yet, many structural changes occur during the wafer bonding process as demonstrated e.g. by the adhesion energy increase with annealing.

Among the different techniques available to study bonding interfaces, high resolution transmission electron microscopy on thinned slices can be used [1,2] but the cross-sections obtained enables hardly one to get an averaged in-plane view of the interface. We shall present here the X-ray reflection technique which combines the large penetration depth of X-rays to their nanometer level sensitivity [3,4]. Interface sensitivity is enhanced due to the use of grazing incidence geometry.

PRINCIPLE OF THE TECHNIQUE

The geometry of the experiment is presented Figure 1. A slice of a few millimeter wide is cut within the bonded wafer assembly and placed onto a goniometer. The X-rays are shone on the side of the sample, are reflected on the interface(s) and exit on the other side. The incidence angles are on the order of a few tenth of a degree and the reflected intensity ranges over several order of magnitudes from 1 to 10⁻⁸ typically. Due to the use of grazing angles, it is necessary to have a rather large reflection surface or a narrow beam to reflect a significant part of it. However, since the beam crosses the full length of one of the bonded material, the sample width should not be too large in order to minimize absorption of X-rays [4]. The answer to these contradictory requirements is to use narrow beams of high energy X-rays (30keV X-rays are typically used).

Synchrotron
side of the
normal inc

D

Fig
is reflected

As for oth
gradients
related to

where λ is
changes v
interfaces
with a phi
distances
varying co
reads as a

where ρ_s
Essentiall
the electr
amplitude

Synchrotron radiation is well suited for that purpose. Note also that reflection from the side of the sample is negligible since the reflection coefficient of materials for X-rays at normal incidence is extremely small.

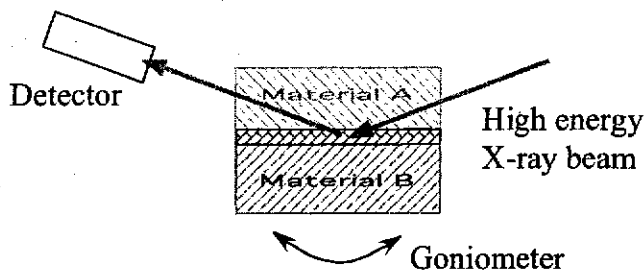


Fig.1 Geometry of the experiment. The beam enters the assembly from one side, is reflected by the bonding interface and exits on the other side of the system.

As for other radiation, the X-ray reflection coefficient of an interface depends on the gradients of index of refraction. In the case of X-rays, the index of refraction n is simply related to the electron density ρ by

$$n = 1 - \frac{\lambda^2}{2\pi} r_e \rho. \quad [1]$$

where λ is the wavelength and r_e is the classical electron radius. Large electron density changes will produce higher reflection amplitudes. In the case where several parallel interfaces are present in a system, the amplitudes reflected by each of them will interfere with a phase factor that depends on their location. As short wavelengths are used, small distances can be measured from this interference. In the case of an electron density varying continuously along the normal to the interface (z), the reflectivity intensity $R(q)$ reads as a function of the incidence angle θ (or the wavevector transfer $q=4\pi\lambda \sin \theta$) as

$$q^4 R(q) = (16\pi^2 r_e^2 \rho_{Si}^2) \left| \int_{-\infty}^{\infty} \frac{\rho'(z)}{\rho_{Si}} \exp(iqz) dz \right|^2 \quad [2]$$

where ρ_{Si} the electron density of silicon and $\rho'(z)$ the derivative of the electron density. Essentially, the reflectivity curve gives the *square modulus* of the Fourier transform of the electron density profile across the interface. Unfortunately the phase of the reflection amplitude is lost which prevents a direct and general inversion of eq[2] to get $\rho(z)$.

- France

interfaces
different
ing such a
structural
adhesion

es, high
] but the
v of the
the large
nsitivity

r wide is
-rays are
the other
reflected
o the use
a narrow
length of
order to
ents is to
y used).

EXPERIMENTAL DATA

We shall consider as a first example of the technique the investigation of a standard Si/Si hydrophilic bonding. Two 4-inch silicon wafers were bonded together after standard wet RCA chemical cleaning. The set of reflection curves is shown Fig.3 for different annealing temperature, the annealing time being constant to 2h.

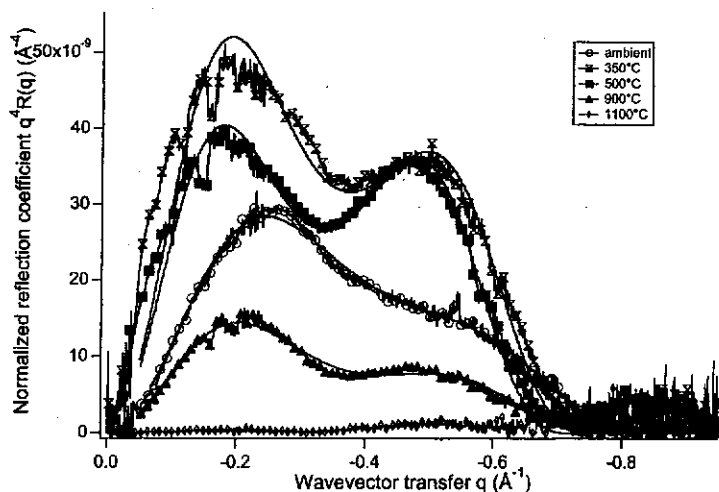


Fig.3: Interfacial reflectivity curves on a Si/Si hydrophilic bonding for different annealing temperatures. The reflection coefficient is multiplied by q^4 in order to remove the standard Fresnel decay of reflection coefficient with angle. The smooth solid lines are fit to the data.

The curves all show a double fringe structure. This double hump is not visible with assemblies including an oxide layer. It is mainly due to the interference between the bonding interface and the native oxide contribution. A simple model including a dip of electron density at the bonding interface and a reduced density layer "box" describing the oxide reproduces the data fairly well (solid lines on fig.3).

Fig.4: Sketch of two boxes

From the fit of these two p

Bonding in

The curves are plotted as a function of the interface. The bonding is between two surface atoms. The surface aspect is due to the roughness of 8Å, which is the order of the contact area. It does the ga

Fig.5 Width of include data

lard Si/Si
standard wet
different

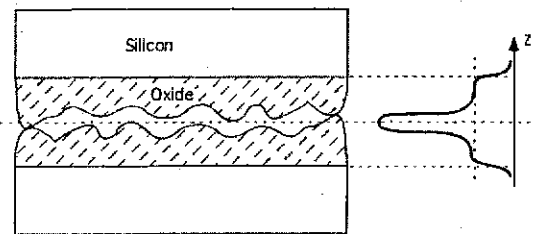


Fig.4: Sketch of the Si/Si bonding assembly: in a first stage the profile is described by two boxes one describing the interface and the other the RCA-induced oxide thin films.

From the fit of such profile to the data it is possible to extract a series of parameters for these two parts of the profile:

Bonding interface

The width and depth of the electron density profile at the bonding interface can be plotted as a function of temperature (Fig.5 and Fig.6). The deficit of electron density at the interface is due to the remaining space that is still present between the wafers after the bonding. Although very flat, silicon surfaces exhibit some roughness and bringing the two surfaces in contact will be opposed by the contact of the highest summits of the surface asperities. The width of the electron deficit is found to be rather large compared to the roughness parameter of all silicon surfaces. Indeed this value is here of the order of 8Å, while the roughness of the silicon surface measured with the same technique is on the order of 2Å. This is due to the fact that only a small fraction of the surface is in actual contact at low temperature. Only when silicon or silicon oxide start to flow (>900°C) does the gap filling occur.

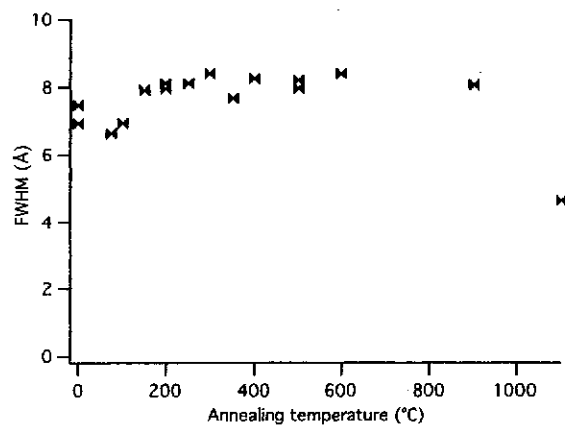


Fig.5 Width of the interface as a function of temperature. This curve and the ones below include data from additional reflectivity experiments not shown on fig.3.

different
to remove
lines are

ible with
ween the
a dip of
ibing the

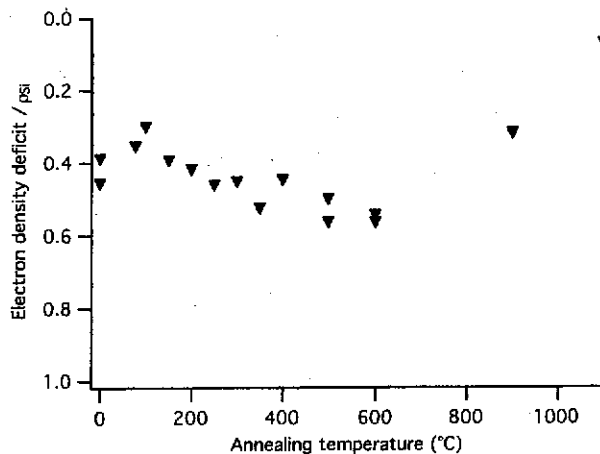


Fig.6 Depth of electron density deficit at the interface normalized to the density of silicon.

The depth of the electron density deficit at the interface slightly increases when heating the sample from room temperature [3]. This first stage can be associated to the water removal. Then at high temperature, the gap seals and this depth decreases again.

Native oxide

The presence of native oxide is clearly evidenced as it is the interference of the interface contribution with this oxide that produces the double bump structure on the reflection curve. From the reflection, information can be obtained on both the thickness and density of this oxide.

These data are plotted on fig. 7 and 8. It can readily be seen that heating the oxide leads to a reduction of its electron density. Simultaneously its thickness increases from 8 to 10Å.

Fig.7: Evolution of the electron density deficit at the interface. The oxide layer (5% water removed) reacts with the oxide thickness.

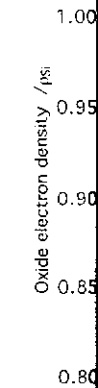


Fig.8 Evolution of the oxide electron density.

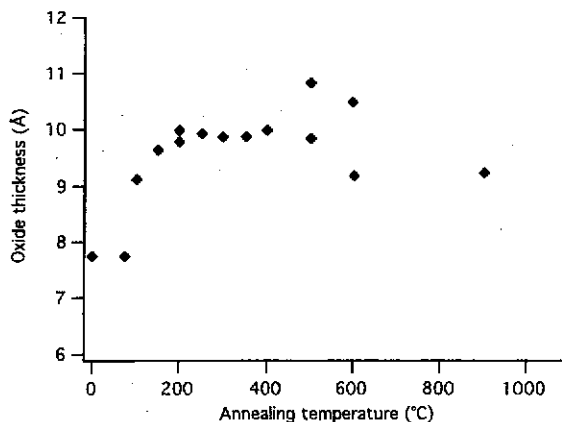


Fig. 7: Evolution of native oxide thickness with annealing temperature. Note the rather sharp increase by 2Å around 100°C

These changes can be associated to the removal of water from this layer and from the interface. A balance of material can be performed from the density change in the oxide layer (5% ρ_{Si}) and in interface gap (10% ρ_{Si}). Assuming these density changes are due to water removal, this would correspond to an equivalent thickness of water of 2.4Å. Reacting with silicon at low temperature, this desorbed water may produce an additional oxide thickness in the observed range (1.8Å).

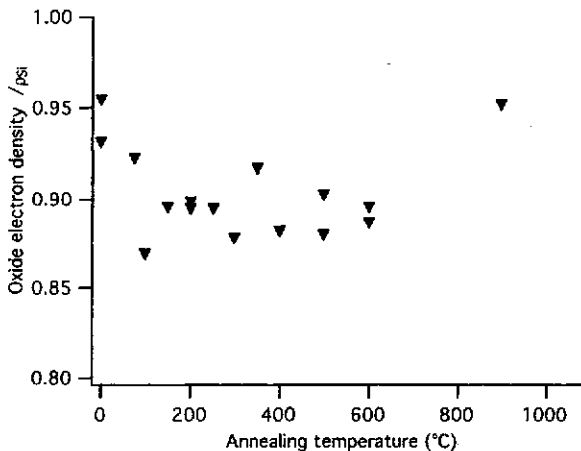


Fig.8 Evolution of native oxide electron density with temperature, normalized to silicon. The oxide experiences a 5% reduction in density when first heated.

ensity of

heating
the water

interface
reflection
density

oxide leads
from 8 to

DIRECT INVERSION OF DATA

In the case of symmetric bonding (Si/Si) or SiO₂/SiO₂ bonding, the electron density profile function $\rho(z)$ is expected to be an even function. Hence, its Fourier transform will be a real function which means that the phase problem reduces to a sign problem in this case. As the amplitude goes to zero when it changes sign, it is possible in this case to directly invert the experimental reflection data to obtain the density profile. This procedure was carried out on the data of figure 3 resulting in the profiles of figure 9.

The different components of the profile are clearly visible whose parameters match the fit parameters very well.

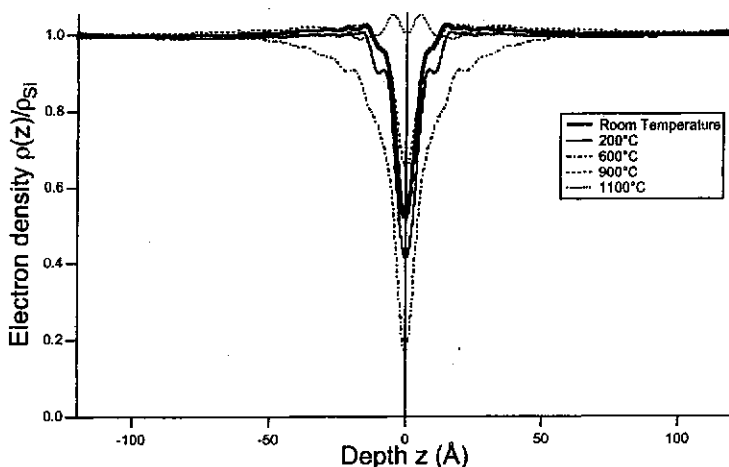


Fig.9: Electron density profile as obtained by direct inversion of the reflection data. The three components of the profile are visible: large electron density deficit at the bonding interface, small shoulders on both part due to native oxide and in some temperature range (600°C profile here) a wide foot that may be the signature of nanometer microvoids

An additional feature that appears using this technique is a rather wide component in the profile, that appears above 200°C up to 600°C. The signature of this larger distance appears (in Fourier space) at small wavevectors (small angles) where indeed some discrepancies remained between the data and the fit using the two-feature description presented above (see fig.3).

The origin of this third feature is not completely clear at the moment. It may be a signature of bubbles observed on acoustic microscopy images in this range of temperature. Assuming they are filled with low density compounds (gas), these nanometric bubbles would cover up to 14% of the total surface area while their vertical extent is on the order of 50Å FWHM.

X-ray interfa
allows the
densities) w
mechanisms
applied to te

Beamtime fi
Facility is ac

1. Q.Y. Tong,
2. A. Reznicek
- Applications V
3. F. Rieutord
- Rev. B, 63, p 1
4. M. Poulser
- Semiconductor
- (2003)
5. B. Bataillon
6. H. Moricea
- Science, Techn
7. H.Moriceau

CONCLUSION

X-ray interfacial reflection is a technique well suited to the study of bonding interfaces. It allows the accurate determination of a series of interface parameters (widths and densities) whose relative evolution with temperature gives some insight as to the mechanisms involved in the sealing of interfaces. Such technique can naturally be applied to test the effect of various surface treatments such as plasma exposure[6,7].

ACKNOWLEDGMENTS

Beamtime from the CRG-Interface beamline at the European Synchrotron Radiation Facility is acknowledged. The CRG-IF beamline is run by CEA and CNRS.

REFERENCES

1. Q.Y. Tong, U. Gösele, *Semiconductor Wafer Bonding Science and Technology*, J. Wiley & Sons (1999)
2. A. Reznicek, R. Scholz, S. Senz, U. Gösele, *Semiconductor Wafer Bonding : Science, Technology and Applications VII*, ECS PV 03-19, 221-232 (2003).
3. F. Rieutord, J. Eymery, F. Fournel, D. Buttard, R. Oeser, O. Plantevin, H. Moriceau, B. Aspar, *Phys. Rev. B*, **63**, p 125408 (2001)
4. M. Poulsen, A. Egebjerg, O. Bunk, M. Nielsen, M.M. Nielsen, R. Feidenhans'l and F. Jensen *Semiconductor Wafer Bonding : Science, Technology and Applications VII*, ECS PV 03-19, 248-258 (2003)
5. B. Bataillou, H. Moriceau, and F. Rieutord, *J. Appl. Cryst.*, vol. 36, pp. 1352-1355, 2003.
6. H. Moriceau, B. Bataillou, C. Morales, A.M. Cartier, F. Rieutord, *Semiconductor Wafer Bonding : Science, Technology and Applications VII*, ECS PV 03-19, 110-117 (2003).
7. H. Moriceau, F. Rieutord, C. Morales, S. Sartori, A. M. Charvet, *this issue*.